

Article

Comparison of Different Anode Materials to Remove *Microcystis aeruginosa* Cells Using Electro-Coagulation–Flotation Process at Low Current Inputs

Thenuwara Arachchige Omila Kasun Meetiayagoda *  and Takeshi Fujino *

Department of Environmental Science and Technology, Graduate School of Science and Engineering, Saitama University, 255 Shimo-okubo, Sakura-ku, Saitama 338-8570, Japan

* Correspondence: 822kasun@gmail.com (T.A.O.K.M.); fujino@mail.saitama-u.ac.jp (T.F.);

Tel.: +81-48-858-9574 (T.F.)

Received: 22 October 2020; Accepted: 13 December 2020; Published: 16 December 2020



Abstract: Cyanobacterial blooms are a threat to the drinking water supply owing to their potential toxicity. Microcystins which are the most widespread cyanotoxins, are mainly produced by *Microcystis* spp. In this study, we cultured *Microcystis aeruginosa* cells in BG-11 medium at 25 °C to investigate the efficiency of the electro-coagulation–flotation process to remove them. Different anode materials (Fe, Al, Cu, and Zn) along with a graphite cathode were compared separately in the 10–100 mA current range in a 0.025 M Na₂SO₄ electrolyte. Turbidity, optical density at 684 nm (OD₆₈₄), OD₇₃₀, Chl-a concentration, and DOC concentration were analyzed to clarify the mechanism by which *M. aeruginosa* cells are removed. The Al anode indicated the highest removal efficiencies in terms of turbidity (90%), OD₆₈₄ and OD₇₃₀ (98%), and Chl-a concentration (96%) within 30 min at 4.0 mA/cm² current density and the lowest average electrode consumption of 0.120 ± 0.023 g/L. The energy consumption of the Al electrode was 0.80 Wh/L. From these results, we found that Al was the best among the anode materials evaluated to remove *M. aeruginosa* cells. However, further studies are required to optimize the Al anode in terms of pH, treatment time, electrode distance, and electrolyte concentration to enhance the removal of *M. aeruginosa* cells.

Keywords: cyanobacteria removal; *Microcystis aeruginosa*; electro-coagulation–flotation; anode material

1. Introduction

Cyanobacterial blooms are one of the major problems worldwide and they can be harmful to the environment, animals, and human health. As a result of rapid oxygen consumption, hypoxic conditions develop, resulting in plant and animal die-off in water bodies [1]. These blooms are a threat to the drinking water supply owing to their potential toxicity and the release of taste and odor compounds such as geosmin and 2-methyl-isoborneol (2-MIB) [2,3]. Generally, cyanobacteria release a large amount of soluble algogenic organic matter (AOM) to the water such as extracellular organic matter (EOM), which is expelled to the water by living algal cells as a product of their metabolic activities, and intracellular organic matter (IOM), which is secreted upon the rupture of cells caused by endogenous or exogenous factors [4–6]. IOM is released as a result of cell lysis when cyanobacteria go through water treatment processes, such as ozonation or chlorination and it is a source of precursor materials for the formation of carcinogenic disinfection by-products (DBPs) combining with chlorine [3,7]. Cyanobacteria have been recognized for decades as a potential source of precursor materials for the formation of DBPs such as trihalomethane (THM) and haloacetic acid (HAA) [3]. The dominant AOMs such as hydrophilic polysaccharides and hydrophobic proteins are

mainly responsible for the fouling of membrane filtration [4]. Therefore, it is important to remove cyanobacterial cells at the start of the water treatment chain.

Cyanotoxins produced by several species of cyanobacteria are another issue. The most widespread cyanotoxins are the peptide toxins called microcystins. There are at least 80 known microcystins, among which microcystin-LR is generally considered the most toxic. *Microcystis* spp. and *Anabaena* spp. are considered the major cyanotoxin-producing cyanobacteria [8,9]. Most of the drinking water guidelines are based on the World Health Organization's provisional value of 1.0 µg/L microcystin-LR for drinking water [1]. Lake Taihu is the third largest freshwater lake in China, where eutrophication promotes *Microcystis* spp. blooms that impair drinking water supplies owing to strong odor, taste, and the presence of microcystin [10].

Cyanobacteria have been removed by conventional treatment techniques such as pre-oxidation by ozone or chlorine dioxide, chemical coagulation, sedimentation, flotation, and filtration using combined membrane technologies. However, there are many problems such as high cost, large amounts of sludge produced, huge energy consumption, and the complexity of treatment processes [11,12]. Recently, the electro-coagulation–flotation (ECF) process has been suggested to be a promising alternative option for cyanobacterial removal [13]. A series of reactions occur during the ECF process. Metal ions are generally released at the sacrificial anode by electrolytic oxidation. Simultaneously, hydrogen and oxygen gas microbubbles are generated at the cathode and anode, respectively. Pollutants combine with the released metal ions to form flocs, which are then removed through the lifting force of microbubbles or sedimentation [14].

The key reactions occurring in the ECF process when aluminum (Al) is used as the anode are shown in Equations (1)–(4) [13,15–17].

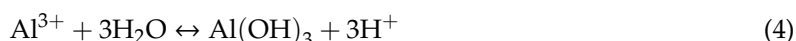
At the anode:



At the cathode:



In solution:



The removal of cyanobacteria through the sedimentation process is challenging because they have a lower density than water owing to gas vacuoles in their cells for regulating the water content [15]. Therefore, the ECF process might be effective and low-cost for cyanobacterial removal.

Only a few studies have focused on the effect of the anode material, mainly Al and/or iron (Fe), on the removal of algae and cyanobacteria by the ECF process. In this research, we compared four anode materials, Fe, Al, copper (Cu), and zinc (Zn), to determine the effect of the anode material on the removal of *Microcystis aeruginosa* cells.

2. Materials and Methods

2.1. Preparation of *Microcystis aeruginosa* Cultures

To prepare new *M. aeruginosa* cultures, we obtained samples from a *M. aeruginosa* monoculture maintained in our laboratory. We used BG-11 medium prepared as described by Rippka et al. [18]. Table 1 shows the ingredients and quantities that were used to prepare the BG-11 medium.

Table 1. Composition of BG-11 medium [18].

Ingredient	NaNO ₃	K ₂ HPO ₄ ·3H ₂ O	MgSO ₄ ·7H ₂ O	CaCl ₂ ·2H ₂ O	Citric Acid	Ferric Ammonium Citrate	EDTA	Na ₂ CO ₃	Trace Metal Mix *
Quantity in 1 L of deionized water	1.5 g	0.04 g	0.075 g	0.036 g	0.006 g	0.006 g	0.001 g	0.02 g	1 mL

* Trace metal mix contains (g/L): H₃BO₃, 2.86 g; MnCl₂·4H₂O, 1.81 g; ZnSO₄·7H₂O, 0.222 g; Na₂MoO₄·2H₂O, 0.390 g; CuSO₄·5H₂O, 0.079 g; Co(NO₃)₂·6H₂O, 0.0494 g.

We used twelve 500 mL Erlenmeyer flasks to culture *M. aeruginosa*. Before inoculation, flasks, rubber stoppers, and the BG-11 medium were sterilized at 121 °C and 0.12 MPa for 20 min in an autoclave (SP300, Yamato Scientific Co., Ltd., Tokyo, Japan) [19]. Each flask was filled with 250 mL of BG-11 medium and closed with a rubber stopper (SILICONE Sterile Stopper, C-40 joint size, AS ONE Corporation, Osaka, Japan) to maintain a proper aeration for their growth. We maintained the cultures in an incubator (LH-55RDS, NK Systems Limited, Tokyo, Japan) at 25 ± 1 °C temperature providing a 12:12 light and dark period and a 60 μmol m⁻²s⁻¹ photon flux of photosynthetically active radiation [20–22]. The flasks with cultures were gently shaken about three times a day to ensure equal exposure of *M. aeruginosa* cells to the light.

Figure 1a,b show the appearance of *M. aeruginosa* cultures at the initial stage and after 14 days of growth, respectively. The initial average pH, turbidity, and optical densities at 684 nm and 730 nm (OD₆₈₄, and OD₇₃₀) of the culture were 7.40 ± 0.06, 6 ± 1 NTU, 0.0309 ± 0.0012, and 0.0322 ± 0.0018, respectively. Cultures showed an S-shaped growth curve and reached an exponential growth within four days. In the exponential phase of growth (14 days after inoculation), about 2.5 L volume of cultures was harvested and gently stirred to obtain a homogenous sample. Before starting the experiments, the pH and electrical conductivity (EC) of samples were adjusted using 0.1 M NaOH or 0.1 M HCl solution and Na₂SO₄, respectively. Table 2 shows the characteristics of *M. aeruginosa* suspensions prepared for the ECF treatment.

**Figure 1.** *M. aeruginosa* cultures. (a) Initial stage (after inoculation) and (b) after 14 days.**Table 2.** Characteristics of *M. aeruginosa* suspensions prepared for electro-coagulation–flotation treatment ($n = 3$).

Parameter	pH	Temp, °C	EC, μS/cm	TDS, mg/L	Turbidity, NTU	OD ₆₈₄	OD ₇₃₀	DOC, mg/L	Chl.-a, μg/mL
Average (S.D.)	7.00 (0.01)	25 (1)	3893.67 (4.73)	3002 (2.65)	166.67 (2.08)	0.9129 (0.0004)	0.8520 (0.0002)	73.85 (1.52)	0.157 (0.013)

2.2. Experimental Setup and Electrode Materials

As shown in Figure 2, all the experiments were carried out at room temperature using 200 mL of *M. aeruginosa* suspension mixed at a speed of 200 rpm using a magnetic stirrer (PC-320, CORNING, Corning, NY, USA). The electrode distance was maintained at 2 cm for each experiment [13]. The effective areas of the anodes and cathode were 25 cm² and 30 cm², respectively. We compared the anode materials along with the graphite cathode separately in the 10 mA–100 mA current range using 0.025 M

Na_2SO_4 electrolyte. The current density was in the range of 0.4–4 mA/cm^2 . The DC voltage was in the range from 1 to 3.8 V. DC power was supplied by a regulated DC digital power supply unit (PMC35-2A, KIKUSUI, Kanagawa, Japan). After conducting each set of experiments, the electrodes were washed with 0.01 M HCl, thoroughly washed with distilled water to remove residuals on the surface, and then weighed.

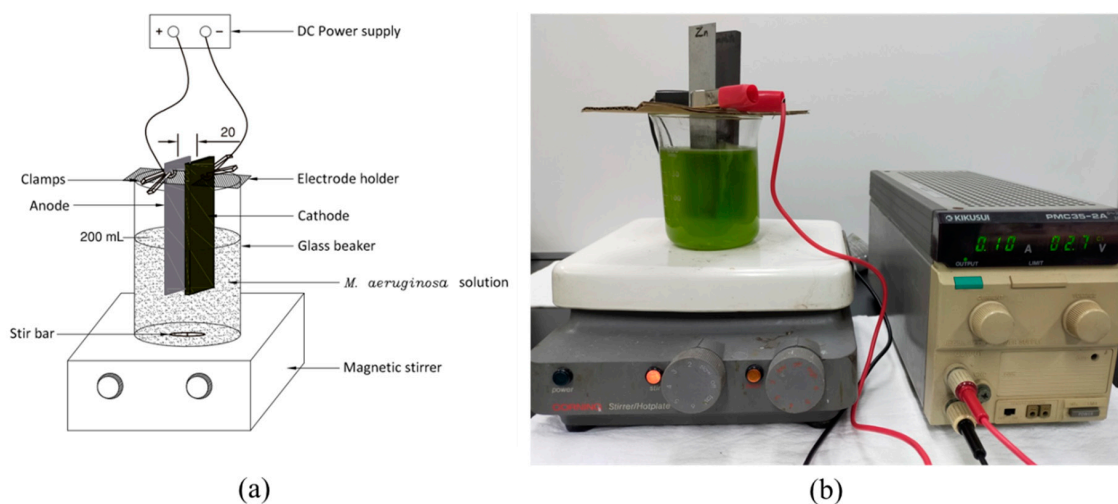


Figure 2. ECF experimental setup for *M. aeruginosa* treatment. (a) Schematic experimental setup (scale 1:10, dimensions are presented in mm). (b) Actual experimental setup. The experiments were conducted in 200 mL glass beakers. The electrodes were connected to a DC power supply (PMC35-2A, KIKUSUI, Kanagawa, Japan) and *M. aeruginosa* suspensions were stirred at 200 rpm using a magnetic stirrer (PC-320, CORNING, Corning, NY, USA).

Anode materials and a graphite cathode were purchased from Ajax Scientific Ltd., Scarborough, ON, Canada. Fe, Al, Cu, and Zn electrodes were selected for the study because these metals are less toxic for humans. All electrodes were rectangular in shape. The details of different anodes are shown in Table 3.

Table 3. Details of different electrodes used for ECF process.

Electrode	Oxidation Potential (E_0), V	Area (W × L), cm^2	Breadth, mm	Weight, g
Fe	0.44	65 (25 × 127)	0.5	14.6
Al	1.66	65 (25 × 127)	0.5	4.3
Cu	−0.52	65 (25 × 127)	0.5	13.9
Zn	0.76	65 (25 × 127)	0.5	14.3
Graphite	-	83.5 (135 × 25)	5.0	25.1

2.3. Analytical Methods

All chemicals used in the study were purchased from FUJIFILM Wako Pure Chemical Industries, Ltd., Osaka, Japan. All physicochemical analyses of water samples were carried out in accordance with standard methods for the examination of water and wastewater [23].

Samples for water quality analyses were collected from 2 cm below the surface using a pipette without disturbing the flocs. Turbidity was measured using a laboratory turbidity meter (2100N, HACH Company, Loveland, CO, USA) and pH was measured using a portable digital meter (Orion 3 star, Thermo Fisher Scientific Co., Ltd., Waltham, MA, USA). EC and total dissolved solids (TDS) were analyzed using a portable conductivity meter (AS710, AS ONE Corporation, Osaka, Japan).

Several studies demonstrated that algae show high absorbance at 684 nm and 730 nm. It was shown that there is a linear relationship between cell count and OD at 684 nm for *M. aeruginosa*

($R^2 > 0.99$) [24,25]. A research carried out by Patel et al. [26] also showed a linear relationship between cell count and OD_{730} for five cyanobacteria species ($R^2 > 0.99$). Therefore, in this study, ODs at 684 nm and 730 nm were analyzed using a UV-Vis spectrophotometer (UV-1280, Shimadzu, Kyoto, Japan). Dissolved organic carbon (DOC) concentration was measured for samples filtered through a 0.45 μm filter paper by a method based on the catalytic oxidation using a TOC analyzer (TOC-2300, Hiranuma Sangyo Co., Ltd., Ibaraki, Japan). Fluorescence microscopy images of *M. aeruginosa* cells were obtained before and after ECF treatment (BZ-X810, KEYENCE Corporation, Osaka, Japan).

The chlorophyll-a (Chl-a) concentration of water samples was measured as described by Zavřel et al. [27]. One milliliter each of sample was dispensed into separate Eppendorf safe-lock tubes and the tubes were centrifuged at $15,000 \times g$ for 7 min in a refrigerated microcentrifuge (TOMY MX-105, Tomy Seiko Co., Ltd., Tokyo, Japan). After discarding the supernatant, 1 mL of methanol was added and the samples were incubated at $+4^\circ\text{C}$ for 20 min to extract pigments from the cells. The samples were again centrifuged at $15,000 \times g$ for 7 min and the absorbance of the supernatant was measured at wavelengths of 665 and 720 nm using a UV-Vis spectrophotometer (UV-1280, Shimadzu, Kyoto, Japan).

Chl-a concentration was determined using Equation (5).

$$\text{Chlorophyll} - a \left(\frac{\mu\text{g}}{\text{mL}} \right) = 12.9447 \times (A_{665} - A_{720}) \quad (5)$$

A_{665} : absorbance at a wavelength of 665 nm

A_{720} : absorbance at a wavelength of 720 nm

Energy consumption was calculated in Wh per L using the Equation (6) reported by Ozyonar et al. [16].

$$\text{Energy consumption} \left(\frac{\text{Wh}}{\text{L}} \right) = \frac{V \times I \times t}{v} \quad (6)$$

V: Voltage (volt)

I: Current (ampere)

t: Operation time (hours)

v: Volume of the treated solution (L)

The dissociation of ions from the anode follows the Faraday's law. The theoretical electrode consumption was calculated in g per L using the Equation (7) given by Ozyonar et al. [16].

$$\text{Electrode consumption}(\text{g/L}) = \frac{I \times t \times M_w}{z \times F \times v} \quad (7)$$

t: Operation time (seconds)

M_w : Molar mass of the anode material (g/mol)

z: Number of electrons involved in the reactions (Al, 3; Fe, 2; Cu, 2; Zn, 2)

F: Faraday's constant (96,485 C/mol)

v: Volume of the treated solution (L).

2.4. Statistical Analyses

All experiments were carried out in triplicate. Statistical analyses were carried out using IBM SPSS Statistics 20.0 software. The removal efficiencies in terms of turbidity, OD_{684} , OD_{730} , Chl-a concentration, and DOC concentration achieved after the ECF treatment were compared among different anode materials by one-way ANOVA post-hoc Tukey HSD (Honestly significant difference) tests to identify the best anode material. All statistical analyses used a significance level of 5% ($p \leq 0.05$).

3. Results

3.1. Comparison of Treated Water Characteristics

The applied current was as low as 10 mA at the start of each experiment and was gradually increased. There were no significant changes observed during the first 30 min of treatment of *M.*

aeruginosa suspensions until the applied current reached 100 mA. Table 4 shows the results of treated water after the 30 min treatment and 30 min settling time at 100 mA applied current.

Table 4. Characteristics of *M. aeruginosa* suspensions treated using different anode materials ($n = 3$).

Electrode	pH	EC, $\mu\text{S/cm}$	TDS, mg/L	Turbidity, NTU	OD ₆₈₄	OD ₇₃₀	DOC, mg/L	Chl.-a, $\mu\text{g/mL}$
Fe	8.88 (0.34)	4283.34 (0.0058)	3266.67 (0.0116)	69.00 (3.61)	0.3945 (0.0171)	0.3578 (0.0113)	45.06 (2.54)	0.0514 (0.0018)
Al	9.77 (0.32)	3776.67 (0.0058)	2890 (0.01)	15.33 (1.53)	0.0168 (0.0047)	0.0164 (0.0047)	44.39 (3.84)	0.0063 (0.0001)
Cu	11.46 (0.48)	3913.34 (0.0153)	3013.34 (0.0153)	37.67 (4.04)	0.0601 (0.0077)	0.0554 (0.0056)	21.85 (2.85)	0.0208 (0.0011)
Zn	10.75 (0.36)	4250 (0.01)	3243.34 (0.0153)	115 (6.56)	0.2160 (0.0098)	0.1915 (0.0090)	43.52 (2.57)	0.0452 (0.0023)

The initial pH was adjusted to 7.00 ± 0.01 before the start of each experiment. The highest and lowest average pHs were recorded for the Cu and Fe anodes: 11.46 ± 0.48 and 8.88 ± 0.34 , respectively. The initial average EC and TDS were $3893.67 \pm 4.73 \mu\text{S/cm}$ and $3002 \pm 2.65 \text{ mg/L}$, respectively, after adding Na_2SO_4 electrolyte. The treatment carried out using the Al anode showed slight reductions in the average EC and TDS to $3776.67 \pm 0.0058 \mu\text{S/cm}$ and $2890 \pm 0.01 \text{ mg/L}$, respectively, but the other anode materials showed slightly higher values than initial values. The Al anode showed the optimal average treated water turbidity, OD₆₈₄, OD₇₃₀, and Chl-a concentration: $15.33 \pm 1.53 \text{ NTU}$, 0.0168 ± 0.0047 , 0.0164 ± 0.0047 , and $0.0063 \pm 0.0001 \mu\text{g/mL}$, respectively. However, the lowest average DOC concentration of $21.85 \pm 2.85 \text{ mg/L}$ was obtained when the Cu anode was used.

Figure 3 shows the appearance of *M. aeruginosa* suspensions before and after treatment using different anode materials. As shown in Figure 3c, the ECF treatment carried out using the Al anode showed the clearest water after the treatment. In the case of using the Fe anode (b), the suspension in the beaker turned yellowish-green at the beginning of the ECF treatment and then changed to yellowish-brown with the time. The suspension treated using the Cu anode (d) appeared a light blue at the final stage of the treatment.

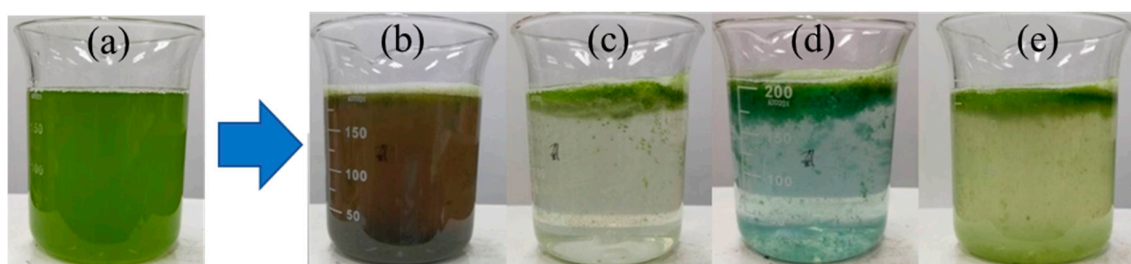


Figure 3. Appearance of suspensions before and immediately after treatment. (a) *M. aeruginosa* suspension before treatment. Suspensions after treatment using (b) Fe anode, (c) Al anode, (d) Cu anode, and (e) Zn anode.

Figure 4 shows the turbidity variation at the initial stage, after 30 min treatment, and after 30 min settling. The initial average turbidity was $166.67 \pm 2.08 \text{ NTU}$. During the 30 min treatment time, the Al and Cu anodes markedly reduced the turbidity up to $38.34 \pm 3.51 \text{ NTU}$ and $53.34 \pm 4.16 \text{ NTU}$, respectively. After the 30 min settling time, water clarity further improved for both Al and Cu electrodes up to $15.34 \pm 1.53 \text{ NTU}$ and $37.67 \pm 4.04 \text{ NTU}$, respectively.

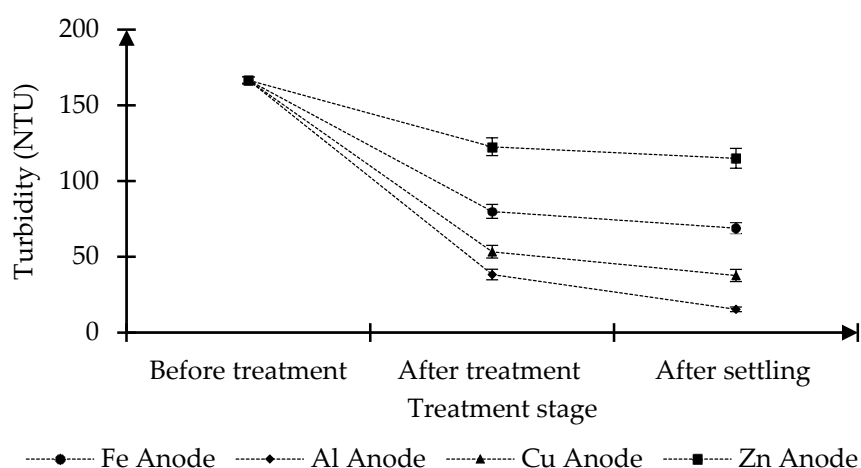


Figure 4. Variation of average turbidity of *M. aeruginosa* suspensions treated using different anode materials at different treatment stages. Error bars represent the standard deviation ($n = 3$).

As shown in Figure 5, the ECF treatment carried out using the Al anode showed the clearest water after the treatment and settling process. In contrast, treatments using Fe, Cu and Zn anodes produced yellowish-brown, light blue, and white cloudy effluents, respectively. Final average EC values were higher than initial EC value in suspensions treated with Fe, Cu and Zn. However, the final EC was $3776.67 \pm 0.0058 \mu\text{S}/\text{cm}$ for the suspension treated with Al anode. It was slightly lower than initial EC value.

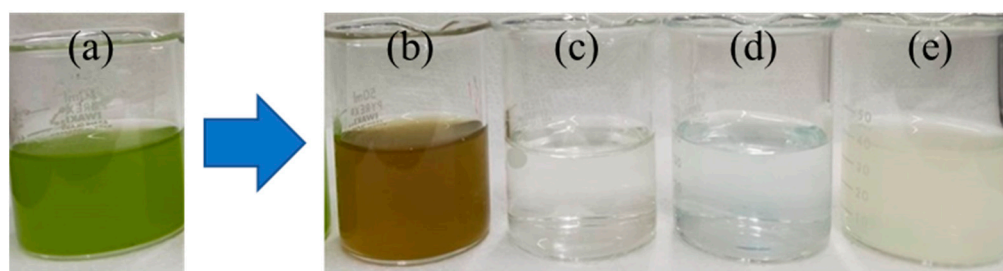


Figure 5. Appearance of suspensions before treatment and after 30 min settling time. (a) *M. aeruginosa* suspension before treatment. Suspensions after settling after treatment using (b) Fe anode, (c) Al anode, (d) Cu anode, and (e) Zn anode.

3.2. Comparison of Removal Efficiency with Respect to Turbidity, OD, Chl-a Concentration, and DOC Concentration among Anode Materials

Figure 6 shows the average removal efficiency as a function of turbidity, OD_{684} , OD_{730} , Chl-a concentration, and DOC concentration for different anode materials. The Al anode showed the highest significant removal efficiency of 91% in terms of turbidity ($F(3,8) = 254.210$, $p < 0.001$) and the highest significant OD_{684} and OD_{730} reduction of 98% ($F(3,8) = 751.252$, $p < 0.001$ and $F(3,8) = 1091$, $p < 0.001$, respectively). The Al anode also showed the highest significant Chl-a removal efficiency of 98% ($F(3,8) = 62.353$, $p < 0.001$). However, the highest significant DOC removal efficiency of 70.41% was observed for the Cu anode ($F(3,8) = 33.751$, $p < 0.001$). The DOC removal efficiency was not significant during the treatment using the Fe, Al, and Zn anodes.

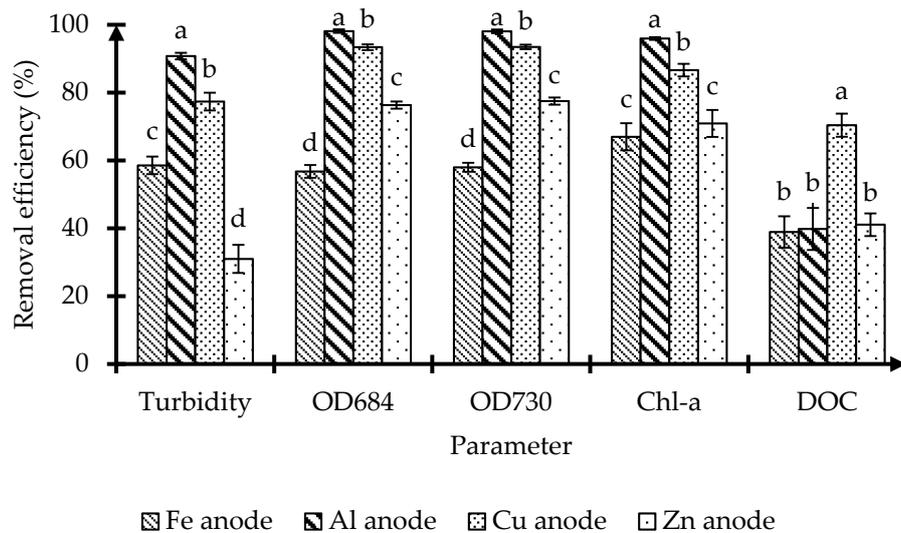


Figure 6. Removal efficiency as a function of turbidity, optical density, Chl-a concentration, and dissolved organic carbon concentration for different anode materials. Error bars represent the standard deviation ($n = 3$). Different superscripts in bars for each parameter indicate a significant difference at 0.05 significant level for different anodes.

3.3. Comparison of Electrode Consumption and Electrical Energy Consumption among Anode Materials

Figure 7 shows the actual and theoretical anode consumptions of different anode materials. The same applied current of 100 mA was used for each experiment using different anodes. The Al and Cu anodes showed the lowest and highest average anode consumptions of 0.120 ± 0.023 and 0.351 ± 0.170 g/L, respectively. However, the theoretical anode consumptions were lower than the actual anode consumptions for Al and Cu anode materials (Figure 7).

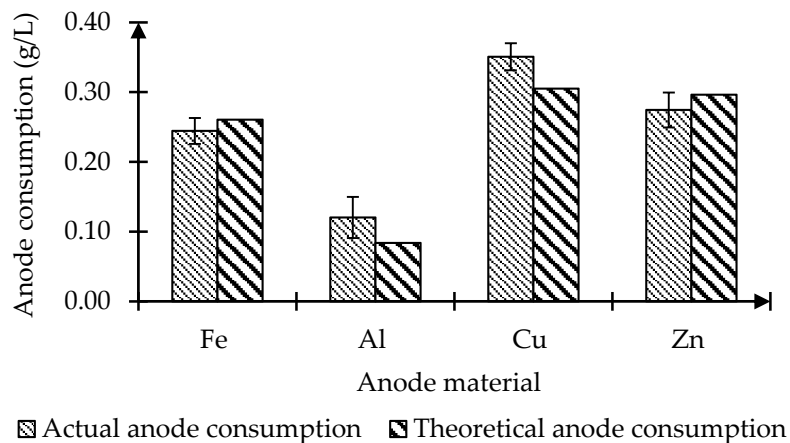


Figure 7. Actual and theoretical anode consumption of different anode materials. Error bars represent the standard deviation ($n = 3$).

Figure 8 shows the electrical energy consumptions of different anode materials. The Zn and Cu anodes showed the lowest and highest electrical energy consumptions of 0.675 and 0.925 Wh/L, respectively. The electrical energy consumptions of the Al and Fe anodes were 0.750 and 0.800 Wh/L, respectively.

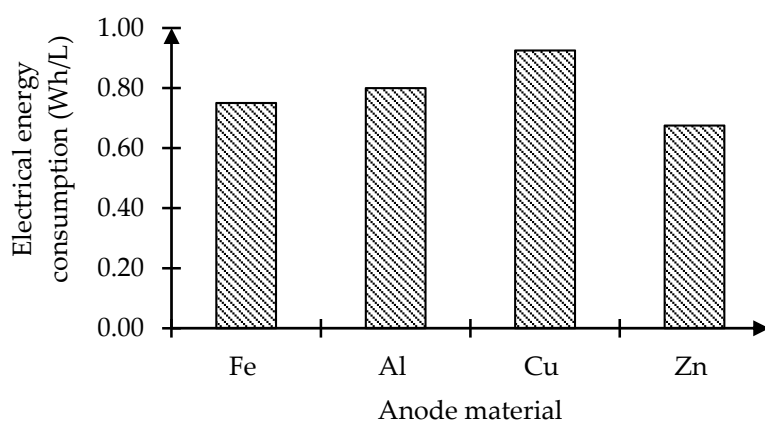


Figure 8. Electrical energy consumptions of different anode materials.

3.4. Appearance of *M. aeruginosa* Cells before and after ECF Treatment Process

Figure 9a,b show the appearance of *M. aeruginosa* cells before and after treatment. Figure 9a shows well-matured *M. aeruginosa* cells after 14 days of incubation with diameters of up to 10 μm . However, cell diameters varied from 5–10 μm . Figure 9b shows the appearance of *M. aeruginosa* cells after ECF treatment. The cells agglomerated and a sheath formed around them.

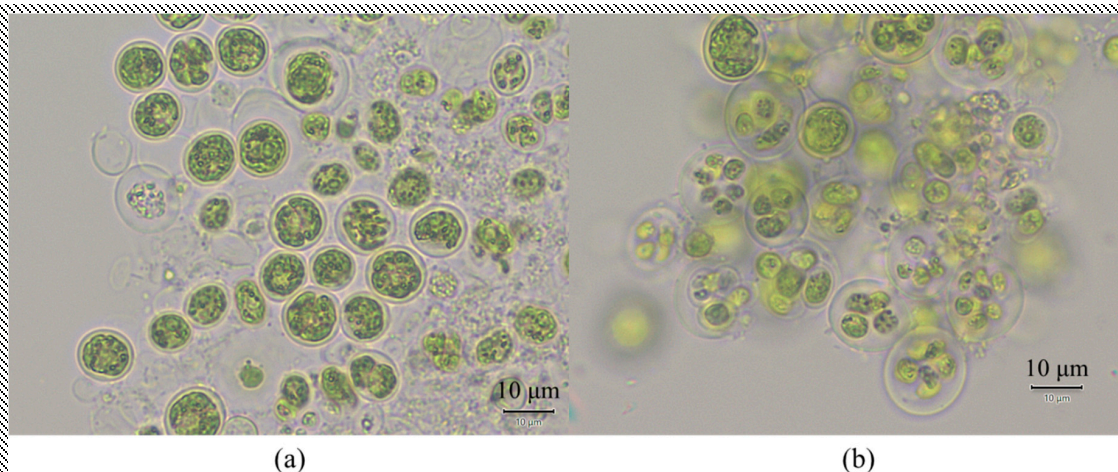


Figure 9. *M. aeruginosa* cells. (a) before and (b) after treatment using Al electrode. The scale bar is 10 μm (captured using a BZ-X810 fluorescence microscope at 44.4 \times magnification).

4. Discussion

In this study, we conducted comparative experiments using Fe, Al, Cu, and Zn as anode materials under the same operational condition for *M. aeruginosa* removal. We used indirect measurements such as turbidity, OD, Chl-a concentration, and DOC concentration to measure *M. aeruginosa* concentrations and AOM at before and after treatment. The Al anode showed the highest removal efficiency in terms of all these parameters except DOC concentration (Figure 6). In this investigation, we started with a current input as low as 10 mA and gradually increased it. There were no any significant changes observed during the first 30 min of treatment in *M. aeruginosa* suspensions until the applied current reached 100 mA. The Al anode showed the highest removal efficiency of 98% for *M. aeruginosa* at 100 mA current and 4 mA/cm² current density for 30 min treatment. A quite similar result was reported by Gao et al. [15]. They demonstrated that 25 min treatment was adequate for 100% *M. aeruginosa* removal at 5 mA/cm² current density. According to Faraday's law, the amount of metal ions released from the anode to the solution increases with increasing current input and electrolysis time. These metal ions incorporated with OH⁻ ions promotes the aggregation of cyanobacterial cells to form flocs [28].

Moreover, the density and size of microbubbles increases and decreases with increasing current input, respectively, which promotes flotation [29].

The initial pH is one of the most critical factors affecting the ECF process [17]. In this study, we maintained the initial pH at 7.00 ± 0.01 . However, the pH increased to alkaline levels after ECF treatment for all the anode materials investigated. This may be due to OH^- ions generated at the cathode as a result of metal ion oxidation at the anode. A similar result was reported by Bleeke et al. [30] for the treatment of *Scenedesmus acuminatus* using the same anode materials. The Cu anode showed the highest final average pH of 11.46 ± 0.48 (Table 4). Tumsri et al. [31] also mentioned that the pH increased markedly during electrolysis when using the Cu anode.

According to Gao et al. [15], at the neutral pH of 7, the amount of aluminum hydroxide is much higher than that of other metal hydroxides. Moreover, a higher current efficiency can be generated by Al electrodes than by Fe, Cu, or Zn electrodes. Owing to hydrolysis reactions, Al ions are hydrolyzed and produce various types of Al species such as monomeric species (e.g., $\text{Al}(\text{OH})^{2+}$ and $\text{Al}(\text{OH})^{2+}$) and polymeric species (e.g., $\text{Al}_{13}(\text{OH})_{34}^{5+}$ and $\text{Al}_{13}\text{O}_4(\text{OH})_{24}^{7+}$). These cationic products react with OH^- ions, which transform into amorphous $\text{Al}(\text{OH})_3$ according to complex precipitation kinetics [17,31].

In this study, the Zn anode showed the lowest electrical consumption (0.675 Wh/L); however, its removal efficiency was lower. The electrical consumption of the Al anode was 0.80 Wh/L (Figure 8) with respect to the lowest anode consumption of 0.12 ± 0.023 g/L (Figure 7) at pH 7 for 30 min treatment with 98% *M. aeruginosa* removal efficiency. Gao et al. [15] reported the electrical consumptions of the Al electrode at different pHs for the complete removal of *M. aeruginosa* by 75 min treatment. The electrical consumption gradually increased with increasing pH: 0.30 Wh/L from pH 4 to 7, 0.53 Wh/L from pH 7 to 9, and 0.60 Wh/L at the initial pH of 10. An experiment carried out for *Chlorella vulgaris* showed that the algae removal efficiency was 96–98.1% for 30 min electrolysis at 6–7 initial pH and 2 mA/cm² current density. The energy consumption was 0.91 Wh/L [31]. At a lower pH, low amount of Al ions is required to remove algal cells owing to charge neutralization. However, when pH is increased, sweep flocculation dominates and a higher amount of Al ions are required to achieve a similar removal efficiency [15]. It is considered that a high efficiency of cyanobacteria/algae removal could be achieved at a low energy consumption under neutral and acidic pH conditions [13,32].

In this study, we used EC and color as indirect measurements especially to identify the excess metal ion concentrations in treated suspensions. Final EC values were higher than initial EC value in suspensions treated with Fe, Cu and Zn respective to dissolution of excess metal ions. However, the final average EC of suspension treated with Al anode was slightly lower than initial EC value. It is realized that there were lower excess aluminum ions in treated suspension. In the case of the Fe anode, the suspensions in the beaker turned yellowish-green at the beginning of the ECF process and gradually changed to yellowish-brown (Figures 3 and 5). These color changes happen owing to the presence of Fe^{2+} and Fe^{3+} ions [15]. Higher turbidity and ODs of treated water were obtained when using the Fe anode than when using the Al and Cu anodes (Table 4). Fe at 0.3 mg/L causes turbidity, changes color, and stains laundry and plumbing fixtures. However, there is usually no conspicuous taste of water at concentrations <0.3 mg/L [33]. The suspensions treated using the Cu anode appeared light blue at the final stage of treatment (Figures 3 and 5). It could be due to Cu^{2+} species produced during electrolytic dissolution [31]. Cu produces a bitter taste and changes the color of water when its concentration is higher than 5 mg/L, and stains laundry fixtures at higher than 1 mg/L [33]. The Zn anode showed the lowest removal efficiency in terms of turbidity as the final solutions appeared white and cloudy as a result of $\text{Zn}(\text{OH})_2$ formation (Figures 3 and 5). Generally, high pHs enhance the generation of these metal hydroxides [34].

We maintained a 30 min settling time for each experiment and measured the turbidity. During the 30 min settling time, the turbidity decreased for all anodes as a result of the sedimentation of flocs (Figure 4). However, the reduction in turbidity during the settling time was very small for the Zn and Fe anodes owing to $\text{Zn}(\text{OH})_2$ precipitation, and of the suspension turned yellowish-brown owing to the oxidation of Fe^{2+} to Fe^{3+} in the presence of oxygen [34,35].

Formation of sludge is a crucial problem as it contains metal ions. Aluminum in sludge can be recovered for subsequent reusing purposes using acidic and alkaline extraction methods. Sulfuric acid (H_2SO_4) is used as the acidification agent in the recovering of the aluminum. This mechanism can also be used to extract other metal ions. Recovery of aluminum in water treatment plant could be a significant approach towards sustainability development [36]. As well as ECF method can use to recover these algae towards the producing of biofuels as a sustainable green energy source.

Regarding the morphology of *M. aeruginosa* cells before and after ECF treatment, we observed that the cells appeared normal with diameters in the range of 5–10 μm ; however, these cells tended to aggregate (Figure 9) after treatment owing to coagulants and the formation of extracellular polysaccharide mucilage around them [37]. In addition, Bakheet et al. [22] reported that more than 30 min electrolysis can disrupt the cell walls and membranes of *M. aeruginosa* cells, resulting in the release of IOM to the medium [4–6]. It is important to remove IOM and EOM precursor materials because they contribute to the formation of carcinogenic DBPs combining with chlorine [3,7]. According to Zhao et al. [38], the EOM and IOM concentrations ranged from very low concentrations to about 100 mg/L depending on the cyanobacterial species. In this research, the initial DOC concentration was 73.85 ± 1.52 mg/L in *M. aeruginosa* suspensions. The Cu anode showed the highest DOC removal efficiency of 70%, whereas the other anodes did not display a significant removal of DOC (Figure 6). However, the Cu anode exhibited the highest anode consumption and energy consumption (Figures 7 and 8). According to Zhou et al. [39] Cu ions can interact with proteins, intercellular nucleic acids, enzymes, and metabolites microbial cells after uptake by them. In case of Al anode, we obtained only a 40% DOC removal efficiency. Guo et al. [40] reported a 38.7% DOC removal efficiency from the IOM of *M. aeruginosa* at 5 mg/L alum dosage. The charge neutralization process involves the elimination of AOM during coagulation owing to the occurrence of extremely negative charges on AOM [6]. However, it is important to carry out these ECF experiments considering the maximum *M. aeruginosa* removal while preventing the release of IOM via cell lysis [41].

5. Conclusions

Al was the best anode material among the materials evaluated (i.e., Fe, Cu, and Zn) to remove *M. aeruginosa* cells at 4.0 mA/cm^2 current density for a 30 min treatment period and a 30 min settling time with the lowest anode consumption. Even though the Cu anode showed the highest DOC removal efficiency, its consumption was high. ECF method with Al anode showed to be a highly effective and rapid method for the removal of *M. aeruginosa* cells. However, further studies are recommended to optimize the Al anode in terms of pH, treatment time, electrode distance, and electrolyte concentration to obtain the maximum removal of *M. aeruginosa* cells. Moreover, the residual aluminum ion concentration, the effect of halide ions on anode dissolution, usage of dimensionally stable anodes could be recommended as important studies for the application purposes.

Author Contributions: Conceptualization, T.A.O.K.M. and T.F.; methodology, T.A.O.K.M. and T.F.; investigation, T.A.O.K.M.; data analysis, T.A.O.K.M.; writing—original draft preparation, T.A.O.K.M.; writing—review and editing, T.F.; visualization, T.F.; supervision, T.F. All authors have read and agreed to the published version of the manuscript.

Funding: This research was funded by the Research Center for Sustainable Development in East Asia, Saitama University (SU-RCSDEA), V3060SR3, and scholarship donation, KF1T253364 (SU).

Acknowledgments: We are indebted to Senavirathna, M.D.H. Jayasanka (SU) for his cooperation with the incubation of *M. aeruginosa* cells.

Conflicts of Interest: The authors declare no conflict of interest.

References

1. Environmental Protection Agency. *Cyanobacteria and Cyanotoxins: Information for Drinking Water Systems*; United States Environmental Protection Agency EPA-810F11001; Office of Water: Washington, DC, USA, 2014; pp. 1–11.
2. Vu, H.P.; Nguyen, L.N.; Zdarta, J.; Nga, T.T.V.; Nghiem, L.D. Blue-Green Algae in Surface Water: Problems and Opportunities. *Curr. Pollut. Rep.* **2020**, *6*, 105–122. [[CrossRef](#)]
3. Wert, E.C.; Rosario-Ortiz, F.L. Intracellular Organic Matter from Cyanobacteria as a Precursor for Carbonaceous and Nitrogenous Disinfection Byproducts. *Environ. Sci. Technol.* **2013**, *47*, 6332–6340. [[CrossRef](#)] [[PubMed](#)]
4. Zhang, X.; Fan, L.; Roddick, F.A. Influence of the characteristics of soluble algal organic matter released from *Microcystis aeruginosa* on the fouling of a ceramic microfiltration membrane. *J. Memb. Sci.* **2013**, *425–426*, 23–29. [[CrossRef](#)]
5. Ghernaout, D. Electrocoagulation Process for Microalgal Biotechnology—A Review. *Djamel Ghernaout Electrocoagul. Process Microalgal Biotechnol. Rev. Appl. Eng.* **2019**, *3*, 85–94. [[CrossRef](#)]
6. Coral, L.A.; Zamyadi, A.; Barbeau, B.; Bassetti, F.J.; Lapolli, F.R.; Prévost, M. Oxidation of *Microcystis aeruginosa* and *Anabaena flos-aquae* by ozone: Impacts on cell integrity and chlorination by-product formation. *Water Res.* **2013**, *47*, 2983–2994. [[CrossRef](#)] [[PubMed](#)]
7. Fang, J.; Yang, X.; Ma, J.; Shang, C.; Zhao, Q. Characterization of algal organic matter and formation of DBPs from chlor(am)ination. *Water Res.* **2010**, *44*, 5897–5906. [[CrossRef](#)]
8. Li, J.; Li, R.; Li, J. Current research scenario for microcystins biodegradation—A review on fundamental knowledge, application prospects and challenges. *Sci. Total Environ.* **2017**, *595*, 615–632. [[CrossRef](#)]
9. Pham, T.L.; Utsumi, M. An overview of the accumulation of microcystins in aquatic ecosystems. *J. Environ. Manag.* **2018**, *213*, 520–529. [[CrossRef](#)]
10. Sakai, H.; Hao, A.; Iseri, Y.; Wang, S.; Kuba, T.; Zhang, Z.; Katayama, H. Occurrence and Distribution of Microcystins in Lake Taihu, China. *Sci. World J.* **2013**, *2013*, 1–7. [[CrossRef](#)]
11. Dong, Y.; Qu, Y.; Li, C.; Han, X.; Ambuchi, J.J.; Liu, J.; Yu, Y.; Feng, Y. Simultaneous algae-polluted water treatment and electricity generation using a biocathode-coupled electrocoagulation cell (bio-ECC). *J. Hazard. Mater.* **2017**, *340*, 104–112. [[CrossRef](#)]
12. Xu, Y.; Yang, J.; Ou, M.; Wang, Y.; Jia, J. Study of *Microcystis aeruginosa* inhibition by electrochemical method. *Biochem. Eng. J.* **2007**, *36*, 215–220. [[CrossRef](#)]
13. An, J.; Li, N.; Wang, S.; Liao, C.; Zhou, L.; Li, T.; Wang, X.; Feng, Y. A novel electro-coagulation-Fenton for energy efficient cyanobacteria and cyanotoxins removal without chemical addition. *J. Hazard. Mater.* **2019**, *365*, 650–658. [[CrossRef](#)] [[PubMed](#)]
14. Mollah, M.; Morkovsky, P.; Gomes, J.; Kesmez, M.; Parga, J.; Cocke, D. Fundamentals, present and future perspectives of electrocoagulation. *J. Hazard. Mater.* **2004**, *114*, 199–210. [[CrossRef](#)] [[PubMed](#)]
15. Gao, S.; Yang, J.; Tian, J.; Ma, F.; Tu, G.; Du, M. Electro-coagulation-flotation process for algae removal. *J. Hazard. Mater.* **2010**, *177*, 336–343. [[CrossRef](#)] [[PubMed](#)]
16. Ozyonar, F.; Karagozoglou, B. Introduction. *Polish J. Environ. Stud.* **2011**, *20*, 173–179.
17. Mouedhen, G.; Feki, M.; Wery, M.D.P.; Ayedi, H.F. Behavior of aluminum electrodes in electrocoagulation process. *J. Hazard. Mater.* **2008**, *150*, 124–135. [[CrossRef](#)]
18. Stanier, R.Y.; Deruelles, J.; Rippka, R.; Herdman, M.; Waterbury, J.B. Generic Assignments, Strain Histories and Properties of Pure Cultures of Cyanobacteria. *Microbiology* **1979**, *111*, 1–61. [[CrossRef](#)]
19. Shirai, M.; Matumaru, K.; Ohotake, A.; Takamura, Y.; Aida, T.; Nakano, M. Development of a Solid Medium for Growth and Isolation of Axenic *Microcystis* Strains (Cyanobacteria). *Appl. Environ. Microbiol.* **1989**, *55*, 2569–2571. [[CrossRef](#)]
20. Islam, M.A.; Beardall, J. Growth and Photosynthetic Characteristics of Toxic and Non-Toxic Strains of the Cyanobacteria *Microcystis aeruginosa* and *Anabaena circinalis* in Relation to Light. *Microorganisms* **2017**, *5*, 45. [[CrossRef](#)]
21. Yuan, R.; Li, Y.; Li, J.; Ji, S.; Wang, S.; Kong, F. The allelopathic effects of aqueous extracts from *Spartina alterniflora* on controlling the *Microcystis aeruginosa* blooms. *Sci. Total Environ.* **2020**, *712*, 136332. [[CrossRef](#)]

22. Bakheet, B.; Islam, M.A.; Beardall, J.; Zhang, X.; McCarthy, D. Effective electrochemical inactivation of *Microcystis aeruginosa* and degradation of microcystins via a novel solid polymer electrolyte sandwich. *Chem. Eng. J.* **2018**, *350*, 616–626. [[CrossRef](#)]
23. AWWA-American Water Works Association. *Standard Methods for the Examination of Water and Wastewater*; American Public Health Association: Washington, DC, USA, 1995.
24. Rajasekhar, P.; Fan, L.; Nguyen, T.; Roddick, F.A. Impact of sonication at 20kHz on *Microcystis aeruginosa*, *Anabaena circinalis* and *Chlorella* sp. *Water Res.* **2012**, *46*, 1473–1481. [[CrossRef](#)] [[PubMed](#)]
25. Zhang, G.; Zhang, P.; Wang, B.; Liu, H. Ultrasonic frequency effects on the removal of *Microcystis aeruginosa*. *Ultrason. Sonochem.* **2006**, *13*, 446–450. [[CrossRef](#)] [[PubMed](#)]
26. Patel, V.K.; Sundaram, S.; Patel, A.K.; Kalra, A. Characterization of Seven Species of Cyanobacteria for High-Quality Biomass Production. *Arab. J. Sci. Eng.* **2018**, *43*, 109–121. [[CrossRef](#)]
27. Zavřel, T.; Červený, J.; Sinetova, M.A. Measurement of Chlorophyll. *Bio-Protocol* **2015**, *5*, e1467. [[CrossRef](#)]
28. Zhu, B.; Clifford, D.A.; Chellam, S. Comparison of electrocoagulation and chemical coagulation pretreatment for enhanced virus removal using microfiltration membranes. *Water Res.* **2005**, *39*, 3098–3108. [[CrossRef](#)] [[PubMed](#)]
29. Holt, P.K.; Barton, G.W.; Wark, M.; Mitchell, C.A. A quantitative comparison between chemical dosing and electrocoagulation. *Colloids Surfaces A Physicochem. Eng. Asp.* **2002**, *211*, 233–248. [[CrossRef](#)]
30. Bleeke, F.; Quante, G.; Winkelmann, D.; Klöck, G. Effect of voltage and electrode material on electroflocculation of *Scenedesmus acuminatus*. *Bioresour. Bioprocess.* **2015**, *2*, 36. [[CrossRef](#)]
31. Tumsri, K.; Chavalparit, O. Optimizing Electrocoagulation-electroflotation Process for Algae Removal. In *2nd International Conference on Environmental Science and Technology IPCBEE*; IACSIT Press: Singapore, 2011; Volume 6, pp. 452–456.
32. Gonzalez-Torres, A.; Putnam, J.; Jefferson, B.; Stuetz, R.M.; Henderson, R.K. Examination of the physical properties of *Microcystis aeruginosa* flocs produced on coagulation with metal salts. *Water Res.* **2014**, *60*, 197–209. [[CrossRef](#)]
33. WHO. *Guideline for Drinking-Water Quality*; Geneva WHO Press: Geneva, Switzerland, 2008; Volume 1, pp. 335–336.
34. Safwat, S.M. Treatment of real printing wastewater using electrocoagulation process with titanium and zinc electrodes. *J. Water Process Eng.* **2020**, *34*, 101137. [[CrossRef](#)]
35. Barışçı, S.; Turkyay, O. Domestic greywater treatment by electrocoagulation using hybrid electrode combinations. *J. Water Process Eng.* **2016**, *10*, 56–66. [[CrossRef](#)]
36. Hassan Basri, M.H.; Mohammad Don, N.N.; Kasmuri, N.; Hamzah, N.; Alias, S.; Azizan, F.A. Aluminium recovery from water treatment sludge under different dosage of sulphuric acid. *J. Phys. Conf. Ser.* **2019**, *1349*, 012005. [[CrossRef](#)]
37. Chen, M.; Tian, L.-L.; Ren, C.-Y.; Xu, C.-Y.; Wang, Y.-Y.; Li, L. Extracellular polysaccharide synthesis in a bloom-forming strain of *Microcystis aeruginosa*: Implications for colonization and buoyancy. *Sci. Rep.* **2019**, *9*, 1251. [[CrossRef](#)] [[PubMed](#)]
38. Zhao, Z. Effects of Drinking Water Treatment Processes on Removal of Algal Matter and Subsequent Water Quality. Ph.D. Thesis, The University of Western Ontario, London, ON, Canada, 2020.
39. Zhou, J.; Wang, T.; Xie, X. Rationally designed tubular coaxial-electrode copper ionization cells (CECICs) harnessing non-uniform electric field for efficient water disinfection. *Environ. Int.* **2019**, *128*, 30–36. [[CrossRef](#)] [[PubMed](#)]
40. Guo, T.; Yang, Y.; Liu, R.; Li, X. Enhanced removal of intracellular organic matters (IOM) from *Microcystis aeruginosa* by aluminum coagulation. *Sep. Purif. Technol.* **2017**, *189*, 279–287. [[CrossRef](#)]
41. Zhao, Z.; Sun, W.; Ray, M.B.; Ray, A.K.; Huang, T.; Chen, J. Optimization and modeling of coagulation-flocculation to remove algae and organic matter from surface water by response surface methodology. *Front. Environ. Sci. Eng.* **2019**, *13*, 75. [[CrossRef](#)]

Publisher’s Note: MDPI stays neutral with regard to jurisdictional claims in published maps and institutional affiliations.



© 2020 by the authors. Licensee MDPI, Basel, Switzerland. This article is an open access article distributed under the terms and conditions of the Creative Commons Attribution (CC BY) license (<http://creativecommons.org/licenses/by/4.0/>).